Eur. J. Mineral.
2016, **28**, 997–1004
Published online 14 June 2016

Zincomenite, $ZnSeO_3$, a new mineral from the Tolbachik volcano, Kamchatka, Russia

IGOR V. PEKOV[1,*], NATALIA V. ZUBKOVA[1], VASILIY O. YAPASKURT[1], SERGEY N. BRITVIN[2], NIKITA V. CHUKANOV[1,3], INNA S. LYKOVA[1,4], EVGENY G. SIDOROV[5] and DMITRY Y. PUSHCHAROVSKY[1]

[1] Faculty of Geology, Moscow State University, 119991 Moscow, Russia
*Corresponding author; e-mail: igorpekov@mail.ru
[2] Department of Crystallography, St Petersburg State University, 199034 St Petersburg, Russia
[3] Institute of Problems of Chemical Physics, Russian Academy of Sciences, 142432 Chernogolovka, Moscow region, Russia
[4] Fersman Mineralogical Museum of Russian Academy of Sciences, 119071 Moscow, Russia
[5] Institute of Volcanology and Seismology, Far Eastern Branch of Russian Academy of Sciences, 683006 Petropavlovsk-Kamchatsky, Russia

Abstract: The new mineral zincomenite, β-$ZnSeO_3$, is found in active fumaroles belonging to the Northern fumarole field at the First scoria cone of the Northern Breakthrough of the Great Tolbachik Fissure Eruption, Tolbachik volcano, Kamchatka, Russia. It is associated with sofiite, sellaite, fluorite, halite, anhydrite, cotunnite, chubarovite, flinteite, *etc*. Zincomenite occurs as tabular, equant or prismatic crystals up to 0.2 mm sometimes combined in clusters up to 0.3 mm across, or interrupted incrustations up to 0.7 × 1 cm overgrowing basalt scoria. Partial to complete pseudomorphs of zincomenite after sofiite are typical. The crystal forms are {101}, {010}, {100} and {013}. T-shaped twins with (012) as twin plane were found. Zincomenite is transparent, colourless, white or pale beige with adamantine lustre. Cleavage and parting were not observed and the fracture is uneven. D_{calc} is 4.760 g cm^{-3}. Zincomenite is optically biaxial (–), α = 1.744(5), β = 1.860(5), γ = 1.875(5). The IR spectrum is reported. The chemical composition (wt.%, electron microprobe data) is: ZnO 42.53, SeO_2 56.67, total 99.20. The empirical formula calculated on the basis of 3 O *apfu* is: $Zn_{1.02}Se_{0.99}O_3$. Zincomenite is orthorhombic, *Pbca, a* = 7.1971(2), *b* = 6.2320(2), *c* = 11.9914(3) Å, *V* = 537.84(2) Å^3 and *Z* = 8. The strongest reflections of the powder X-ray diffraction pattern [*d*,Å(*I*)(*hkl*)] are: 4.612(26)(102), 3.601(77)(200), 3.119(48)(210), 3.048 (38)(113), 3.014(100)(211, 021), 2.996(56)(004), 2.771(19)(123, 104, 212), 2.459(23)(213, 023), 2.311(20)(123, 221, 204), and 2.162 (19)(214, 024). Zincomenite is a representative of the $CuSeO_3$ structure type. Its crystal structure, solved from single-crystal X-ray diffraction data (*R* = 0.0188), contains layers formed by Zn_2O_8 dimers (consisting of edge-sharing ZnO_5 trigonal bipyramids; each dimer shares four vertices with the neighbouring ones) linked *via* $(SeO_3)^{2-}$ groups (with Se^{4+} in trigonal pyramidal coordination) to form an open framework. The mineral is named in allusion to its chemical composition: zinc selenite (the Greek μηναζ means *moon*, indicating selenium).

Key-words: crystal structure, fumarole sublimate, Kamchatka, new mineral, Tolbachik volcano, zinc selenite, zincomenite.

Introduction

Selenites are typical for sublimates of active fumaroles located at the First and Second scoria cones of the Northern Breakthrough of the Great Tolbachik Fissure Eruption (NB GTFE), Tolbachik volcano, Kamchatka Peninsula, Far-Eastern Region, Russia (55°41′N 160° 14′E, 1200 m asl). Tolbachik is probably a world "record-holder" in the diversity of oxygen-bearing selenium minerals. Ten species are endemic for its fumarole fields, including eight copper-bearing selenites with additional anions O^{2-} and Cl^- and two zinc selenites. They are the dimorphous georgbokiite and parageorgbokiite $Cu_5O_2(Se^{4+}O_3)_2Cl_2$ (Vergasova *et al*., 1999a, 2007), chloromenite $Cu_9O_2(Se^{4+}O_3)_4Cl_6$ (Vergasova *et al*., 1999b), nicksobolevite $Cu_7O_2(Se^{4+}O_3)_2Cl_6$ (Vergasova *et al*., 2014), ilinskite $NaCu_5O_2(Se^{4+}O_3)_2Cl_3$ (Vergasova *et al*., 1997), burnsite $KCdCu_7O_2(Se^{4+}O_3)_2Cl_9$ (Krivovichev *et al*., 2002), allochalcoselite $PbCu^+Cu^{2+}{}_5O_2(Se^{4+}O_3)_2Cl_5$ (Vergasova *et al*., 2005), prewittite $KPb_{1.5}ZnCu_6O_2(Se^{4+}O_3)_2Cl$ (Shuvalov *et al*., 2013), sofiite $Zn_3(Se^{4+}O_3)Cl_2$ (Vergasova *et al*., 1989), and a new mineral described in the present paper, zincomenite β-$ZnSe^{4+}O_3$. Two Pb–Se–O minerals are also known from the Tolbachik fumaroles, namely molybdomenite $PbSe^{4+}O_3$ (Serafimova *et al*., 1994) and recently found olsacherite $Pb_2(Se^{6+}O_4)(SO_4)$ (our unpublished data).

Zincomenite (Cyrillic: цинкоменит) is named in allusion to its chemical composition: zinc selenite (the Greek

DOI: 10.1127/ejm/2016/0028-2564
0935-1221/16/0028-2564 $ 3.60

μηναζ means *moon*, indicating selenium). Both the new mineral and its name have been approved by the IMA Commission on New Minerals, Nomenclature and Classification (IMA 2014-014). The type specimen is deposited in the systematic collection of the Fersman Mineralogical Museum of the Russian Academy of Sciences, Moscow, with the catalogue number 94377.

Occurrence and general appearance

Specimens with the new mineral were collected by us in July 2013 in active fumaroles belonging to the Northern fumarole field located at the northern slope of the crater of the First scoria cone of the NB GTFE. This scoria cone is a monogenetic volcano about 300 m high and approximately 0.1 km^3 in volume formed in 1975 and situated 18 km SSW of the active volcano Ploskiy Tolbachik (Fedotov & Markhinin, 1983). The First scoria cone shows fumarolic activity to present day: numerous gas vents with temperatures up to 300 ºC are observed around and inside its crater.

The mineralized fumarole chambers in which zincomenite was found occur at 0.1 to 0.3 m depths below day surface. Our measurements therein, performed using chromel-alumel thermocouple when collecting, showed temperatures of 180–200 ºC. The walls of the chambers are partially covered by sublimate incrustations mainly consisting of sellaite, fluorite, halite and anhydrite. Minerals of lead, zinc, manganese and selenium, which determine the geochemical specialization of the Northern fumarole field, overgrow these white to grey massive crusts or red-brown porous basalt scoria altered by volcanic gas. Cotunnite $PbCl_2$, sofiite $Zn_3(Se^{4+}O_3)Cl_2$ and, sporadically, flinteite K_2ZnCl_4 (Pekov *et al.*, 2015b) are common here. Subordinate minerals are zincomenite $ZnSeO_3$, chubarovite $KZn_2(BO_3)Cl_2$ (Pekov *et al.*, 2015a), anglesite $PbSO_4$, challacolloite KPb_2Cl_5, olsacherite $Pb_2(Se^{6+}O_4)(SO_4)$, saltonseaite $K_3NaMnCl_6$, hollandite $Ba(Mn^{4+}{}_6Mn^{3+}{}_2)O_{16}$, bixbyite Mn_2O_3, as well as jakobssonite $CaAlF_5$, sylvite, hematite and baryte. Cryobostryxite $KZnCl_3 \cdot 2H_2O$ (Pekov *et al.*, 2015c), leonardsenite $MgAlF_5 \cdot 2H_2O$, ralstonite, gypsum, vernadite and opal are formed in upper parts of the fumarole systems and are products of the supergene alteration of sublimate minerals.

Zincomenite occurs as tabular, equant or prismatic (elongated along [010]), rarely lamellar, crystals (Fig. 1), usually up to 0.05 mm, very rarely up to 0.2 mm across. They are typically crude, more rarely perfect. The crystal forms are {101}, {010}, {100} and {013} (Fig. 2a–c). On some crude crystals, the presence of other faces belonging to the {*h*0*l*} zone (in particular, {001}) could be assumed. T-shaped twins with (012) as twin plane were found (Fig. 1a, b and 2d). The {010} faces of crystals are smooth, mirror-like, while the faces of the {*h*0*l*} zone, especially {100}, can be coarsely striated (striation along [010]), "ribbed" (Fig. 1). Dense crystal clusters (Fig. 1e) up to 0.3 mm across are common. Chain-like crystal groups up to 0.25 mm long (Fig. 1f) occur in some specimens.

Thin, interrupted incrustations of zincomenite, covering the surface of basalt scoria, are up to 0.7 cm × 1 cm in area. Microcrystalline crusts of the new mineral also cover, commonly with partial or sometimes full replacement, rosette- or flower-like clusters (up to 1 mm across) of sofiite (Fig. 3), the most abundant selenium mineral in these fumaroles. Some such specimens are very rich in zincomenite, with areas up to several cm^2 "sprinkled" with numerous partial to complete pseudomorphs of the new mineral after sofiite.

Physical properties and optical data

Zincomenite is transparent, colourless in separated crystals and colourless, white or pale beige in aggregates, with white streak and adamantine lustre. Microcrystalline aggregates are sparkling (Fig. 3). The mineral is non-fluorescent under ultraviolet light or an electron beam. Zincomenite is brittle. Its hardness could not be measured correctly because of the tiny size of individuals and the friable character of crusts. Cleavage or parting was not observed and the fracture is uneven. Density could not be measured because monomineralic, massive particles of zincomenite are too small for volumetric methods and because of lack of heavy liquids of necessary density. The calculated density is 4.760 g cm^{-3}.

Zincomenite is optically biaxial (–), $\alpha = 1.744(5)$, $\beta = 1.860(5)$, $\gamma = 1.875(5)$ (589 nm); $2V_{meas}$ is medium and $2V_{calc} = 38°$. Dispersion of optical axes was not observed. Under the microscope the mineral is colourless and non-pleochroic.

Infrared spectroscopy

The infrared (IR) absorption spectrum of zincomenite was recorded for a powdered sample mixed with anhydrous KBr and pelletized. The pellet was analyzed using an ALPHA FTIR spectrometer (Bruker Optics) at a resolution of 4 cm^{-1}, with 16 sampling scans. The IR spectrum of a pure KBr disc was subtracted from the overall spectrum.

The absorption bands in the IR spectrum of zincomenite (Fig. 4) (cm^{-1}, s – strong band, w – weak band) are: 845, 826, 818, 758, 724s, 697s, 532, 483w. Numerous weak and narrow bands above 1200 cm^{-1} correspond to bending vibrations of atmospheric water. Due to the insufficient amount of substance, scattering and atmospheric noise we were not able to obtain an IR spectrum of acceptable quality in the region above 1800 cm^{-1}. The spectrum of zincomenite is close to that of its synthetic analogue, which shows the strongest bands at ~850, ~820, ~760, ~720, ~690 and ~530 cm^{-1} (Bachvarova-Nedelcheva *et al.*, 2005). Bands in the ranges 690–850 and 450–550 cm^{-1} correspond to stretching and bending vibrations, respectively, of the SeO_3^{2-} anion. This is characteristic for selenite minerals in general (Chukanov, 2014; Chukanov & Chervonnyi, 2016).

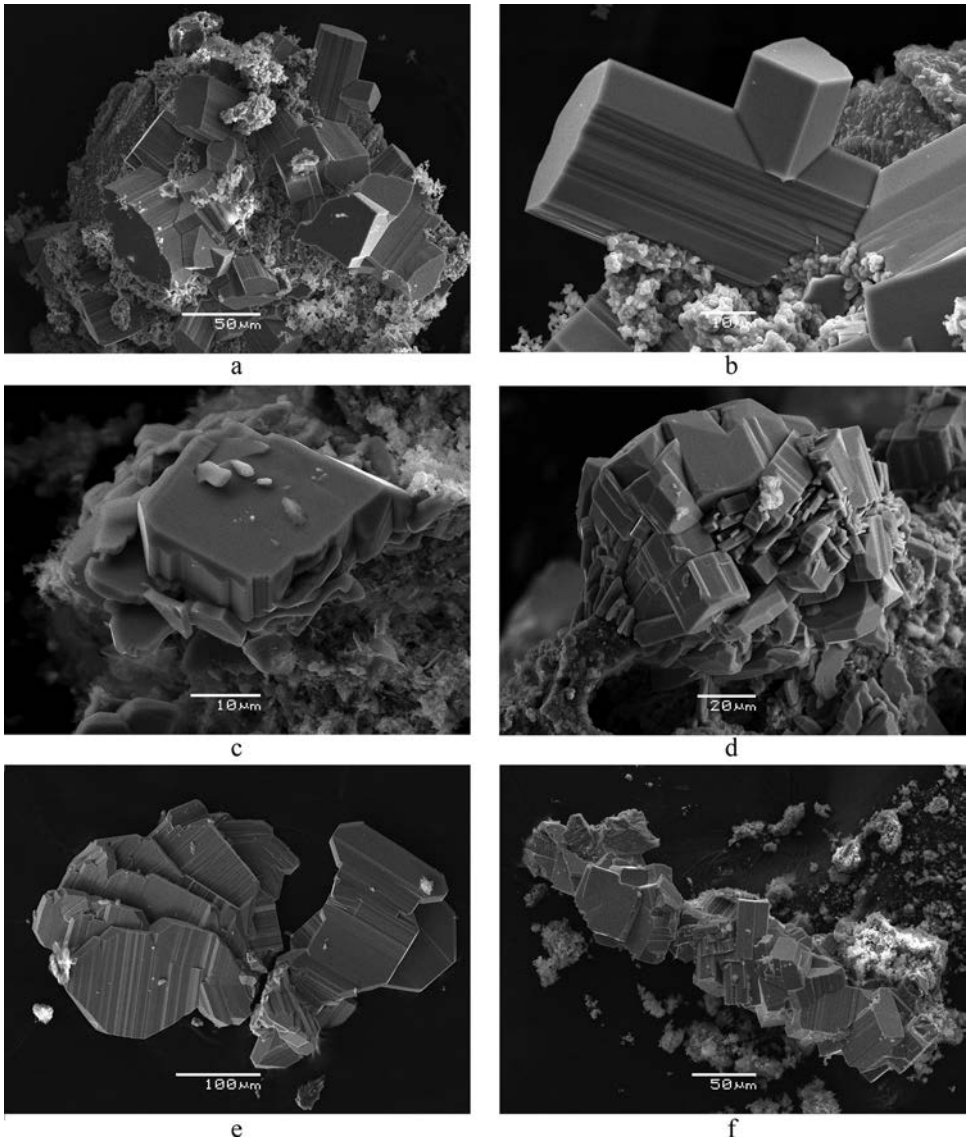

Fig. 1. Morphology of crystals and aggregates of zincomenite: a – prismatic crystals and T-like twin with (012) as twin plane; b – the same twin, enlarged; c – tabular crystal; d – cluster consisting of equant and tabular crystals; e – fan-shaped aggregate of distorted, lamellar crystals; f – chain-like intergrowth of crystals of different shapes. Scanning electron microscope images (secondary electrons).

Bending vibrations of the SeO_3^{2-} anion are possibly combined with stretching vibrations of ZnO_5 polyhedra to generate mixed normal modes. Splitting of the bands of the Se^{4+}–O stretching vibrations reflects distortion of the SeO_3 groups in the mineral (see below), as well as in synthetic β-$ZnSeO_3$ (Bensch & Günther, 1986; Hawthorne *et al*., 1986). Additional splitting may be due to Fermi resonance with overtones of low-frequency lattice modes.

Bands due to SeO_4^{2-} are not observed in the IR spectrum of zincomenite (the strongest bands of the selenate ion are usually observed in the ranges 830–880 and 410–440 cm^{-1}: Georgiev *et al*., 2010). The absence of absorptions in the range 900-1800 cm^{-1} indicates the absence of O–H, C–O and B–O covalent bonds.

Chemical composition

The chemical composition of zincomenite was studied using a Jeol JSM-6480LV scanning electron microscope equipped with an INCA-Wave 500 wavelength-dispersive spectrometer (Laboratory of Analytical Techniques of High Spatial Resolution, Dept. of Petrology, Moscow State University), with an acceleration voltage of 20 kV, a beam current of 20 nA, and a 3 μm beam diameter. Synthetic ZnSe was used as a probe standard for both Zn and Se. Contents of other elements with atomic numbers higher than carbon are below their detection limits.

The chemical composition of zincomenite (average of five spot analyses; wt.%, ranges are in parentheses) is:

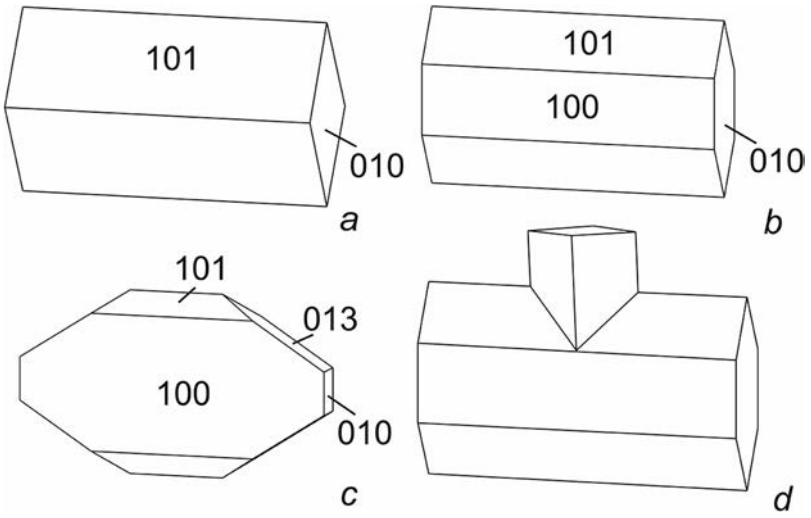

Fig. 2. Idealized crystals (a–c) and twin with (012) as twin plane (d) of zincomenite.

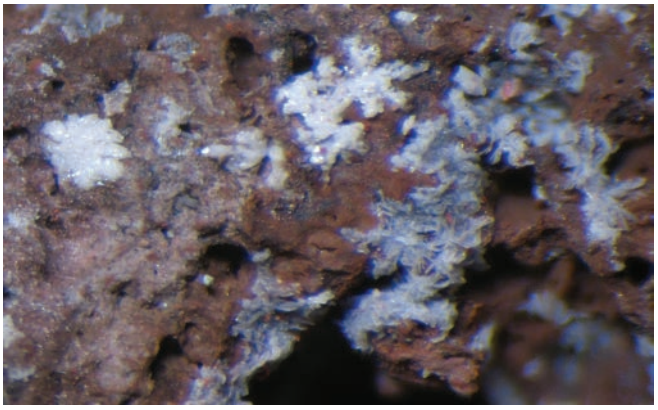

Fig. 3. White, sparkling pseudomorphs of zincomenite after flower-like clusters of sofiite on basalt scoria altered by fumarole gas. Greyish aggregates of lamellar crystals of almost unaltered sofiite are shown in the right and bottom parts of the photograph. Field of view: 3.4 mm. Photo: I.V. Pekov & A.V. Kasatkin.

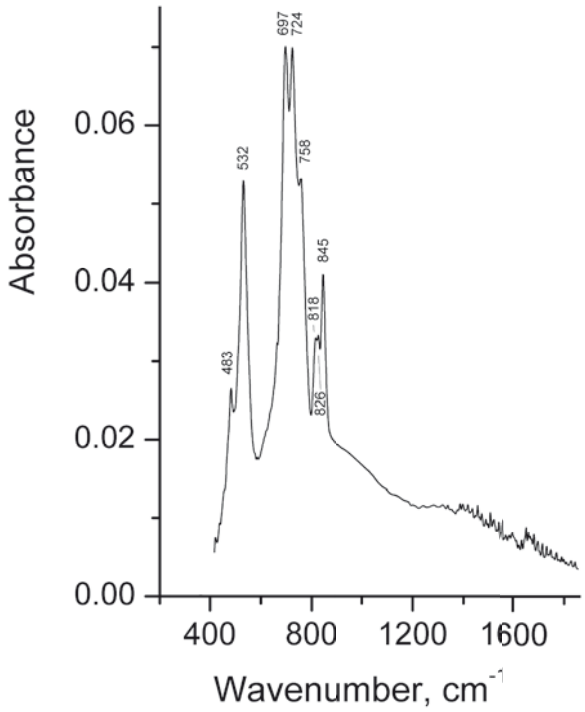

Fig. 4. The powder IR absorption spectrum of zincomenite.

ZnO 42.53 (42.08–43.15), SeO_2 56.67 (55.49–57.58), total 99.20.

The empirical formula calculated on the basis of 3 O atoms per formula unit (*apfu*) is: $Zn_{1.02}Se_{0.99}O_3$. The idealized formula is $ZnSeO_3$, which requires ZnO 42.31, SeO_2 57.69, total 100.00 wt%.

The Gladstone-Dale compatibility index is: $1 - (K_p/K_c) = 0.031$, excellent.

X-ray crystallography and crystal structure

Powder X-ray diffraction data of zincomenite (Table 1) were collected with a Rigaku R-AXIS Rapid II single-crystal diffractometer equipped with cylindrical image-plate detector using Debye-Scherrer geometry (Co$K\alpha$ radiation, d = 127.4 mm). The orthorhombic unit-cell parameters refined from the powder data are: a = 7.199(1), b = 6.238(1), c = 12.006(2) Å and V = 539.2(2) Å^3.

The single-crystal X-ray diffraction study of zincomenite was carried out using an Xcalibur S diffractometer equipped with a CCD detector. A full sphere of three-dimensional data was collected. The measured intensities were corrected for Lorentz, background, polarization and absorption effects. Data reduction

Table 1. Powder X-ray diffraction data of zincomenite.

I_{obs}	d_{obs}	I_{calc}, Å*	d_{calc}, Å**	*h k l*
3	6.00	2	5.996	002
26	4.612	26	4.607	102
3	4.389	2	4.385	111
12	3.706	10	3.704	112
77	3.601	95	3.599	200
48	3.119	65	3.116	210
38	3.048	45	3.048	113
100	3.014	27, 100	3.016, 3.016	211, 021
56	2.996	69	2.998	004
19	2.771	7, 16, 8	2.781, 2.767, 2.765	121, 104, 212
7	2.531	10	2.529	114
23	2.459	17, 29	2.458, 2.458	213, 023
20	2.311	1, 35, 13	2.326, 2.311, 2.303	123, 221, 204
3	2.202	4	2.201	311
19	2.162	33, 3	2.160, 2.160	214, 024
2	2.138	1	2.137	115
13	2.099	24	2.097	312
2	2.031	3	2.029	223
2	2.001	4	1.999	006
3	1.970	6	1.969	131
4	1.955	8	1.953	313
9	1.901	5, 12, 6	1.901, 1.901, 1.894	215, 025, 132
6	1.875	2, 9	1.877, 1.873	321, 304
2	1.854	1	1.852	224
4	1.840	2, 5	1.840, 1.838	116, 125
7	1.800	13	1.799	230
5	1.782	2, 9	1.786, 1.779	133, 231
4	1.728	7, 2	1.729, 1.723	410, 402
5	1.714	6, 9	1.717, 1.711	323, 411
6	1.682	2, 13	1.682, 1.681	216, 225
3	1.663	7	1.661	134
6	1.649	15	1.641	233
7	1.612	16	1.610	117
4	1.588	6	1.587	413
7	1.559	10, 3	1.558, 1.557	040, 331
6	1.544	1, 8	1.543, 1.543	404, 234
4	1.536	4	1.534	135
5	1.521	1, 9	1.524, 1.519	226, 332
7	1.500	1, 4, 1, 9	1.501, 1.501, 1.499, 1.498	217, 027, 008, 414
5	1.493	3, 5	1.491, 1.490	316, 325
4	1.470	3, 4	1.470, 1.467	127, 108
3	1.453	4	1.452	423
7	1.431	6, 12	1.430, 1.428	240, 118
1	1.414	2	1.412	136
6	1.402	5, 10	1.402, 1.400	415, 502
4	1.384	1, 9	1.384, 1.383	208, 044
3	1.367	5	1.366	512
4	1.362	3, 4	1.361, 1.360	317, 430
2	1.339	3	1.337	406
2	1.315	2	1.314	335
3	1.308	2	1.307	425
6	1.301	8, 3, 1	1.300, 1.299, 1.299	137, 521, 341
4	1.292	7	1.291	244
7	1.273	9, 6, 1	1.273, 1.271, 1.270	327, 308, 514
5	1.242	7, 3	1.242, 1.241	523, 237
3	1.237	4, 2	1.238, 1.235	434, 336
1	1.228	1, 1	1.228, 1.225	245, 029
1	1.211	2, 1	1.211, 1.208	515, 129
3	1.200	6, 3	1.199, 1.198	138, 344
1	1.184	2	1.183	435
2	1.179	2, 2	1.178, 1.177	250, 531
3	1.175	4	1.174	153

*Only reflections with intensities ≥ 1 are included; **calculated from the single-crystal data.

Table 2. Crystal data, data collection information and crystal-structure refinement details for zincomenite.

Formula	$ZnSeO_3$
Formula weight	192.33
Temperature, K	293(2)
Radiation and w avelength, Å	Mo*K*α; 0.71073
Crystal system, space group, *Z*	Orthorhombic, *Pbca*, 8
Unit-cell dimensions, Å	*a* = 7.1971(2) *b* = 6.2320(2) *c* = 11.9914(3)
V, Å^3	537.84(3)
Absorption coefficient μ, mm^{-1}	22.412
F_{000}	704
Crystal size, mm	0.06 × 0.08 × 0.15
Diffractometer	Xcalibur S CCD
θ range for data collection, °	3.40 – 30.51
Index ranges	$-10 \le h \le 10$, $-8 \le k \le 8$, $-17 \le l \le 17$
Reflections collected	10667
Independent reflections	823 (R_{int} = 0.0480)
Independent reflections with $I > 2\sigma(I)$	786
Structure solution	direct methods
Data reduction	CrysAlisPro, version 1.171.35.21 (Agilent Technologies, 2012)
Absorption correction	analytical numeric absorption correction using a multifaceted crystal model based on expressions derived by Clark & Reid (1995).
Refinement method	full-matrix least-squares on F^2
Number of refined parameters	47
Final *R* indices [$I > 2\sigma(I)$]	*R*1 = 0.0188, w*R*2 = 0.0393
R indices (all data)	*R*1 = 0.0206, w*R*2 = 0.0399
GoF	1.153
Largest diff. peak and hole, e/Å^3	0.486 and -0.554

was performed using CrysAlisPro Version 1.171.35.21 (Agilent Technologies, 2012). The crystal structure of the mineral was solved by direct methods and refined using the SHELX-97 software package (Sheldrick, 2008) to R = 0.0188 for 786 independent reflections with $I > 2\sigma(I)$. The crystal data and the experimental details are presented in Table 2, atom coordinates and displacement parameters in Table 3, selected interatomic distances in Table 4 and bond-valence calculations in Table 5.

Zincomenite as well as its synthetic full analogue β-$ZnSeO_3$ belong to a family of selenites related to the $CuSeO_3$ structure type (Kohn *et al*., 1976; Bensch & Günther, 1986; Hawthorne *et al*., 1986). The crystal structure of the new mineral is based upon an open framework built by the (001) zinc–oxygen polyhedral layers linked *via* isolated $(SeO_3)^{2-}$ groups where Se^{4+} occurs in its usual trigonal pyramidal coordination (Fig. 5a and b). The zinc–oxygen layers are formed by Zn_2O_8 dimers consisting of edge-sharing ZnO_5 trigonal

Table 3. Atom coordinates and displacement parameters (in Å^2) in the structure of zincomenite.

Atom	*x*	*y*	*z*	U_{eq}	U_{11}	U_{22}	U_{33}	U_{23}	U_{13}	U_{12}
Zn	0.60746(4)	0.36479(5)	0.59581(3)	0.01045(9)	0.01228(16)	0.01033(16)	0.00873(16)	0.00089(11)	-0.00036(11)	-0.00192(11)
Se	0.54450(3)	0.38808(4)	0.85748(2)	0.00807(8)	0.00923(13)	0.00696(13)	0.00801(13)	0.00031(8)	0.00067(9)	-0.00042(9)
O(1)	0.6512(3)	0.0163(3)	0.59326(17)	0.0112(4)	0.0108(8)	0.0088(9)	0.0141(9)	0.0014(7)	0.0033(7)	-0.0006(7)
O(2)	0.5308(3)	0.3410(3)	0.43451(16)	0.0132(4)	0.0215(10)	0.0083(9)	0.0100(9)	-0.0011(7)	-0.0042(8)	0.0022(7)
O(3)	0.4661(3)	0.2980(3)	0.73398(16)	0.0123(4)	0.0180(9)	0.0117(9)	0.0072(9)	-0.0015(7)	0.0010(7)	-0.0018(8)

Table 4. Selected interatomic distances (Å) in the structure of zincomenite

Zn	Se
– O(1) 1.9774(19)	– O(3) 1.6812(19)
– O(3) 1.9884(19)	– O(2) 1.703(2)
– O(2) 2.017(2)	– O(1) 1.7234(19)
– O(2) 2.118(2)	<Se – O> 1.702
– O(1) 2.1948(19)	
<Zn – O> 2.059	

Table 5. Bond valence calculations for zincomenite. Parameters are taken from Brese & O'Keeffe (1991) .

	Zn	Se	Σ
O(1)	0.48	1.27	2.02
	0.27		
O(2)	0.43	1.34	2.10
	0.33		
O(3)	0.46	1.42	1.88
Σ	1.97	4.03	

bipyramids; each dimer shares four vertices with the neighbouring ones (Fig. 5b).

The Zn-centred trigonal bipyramids were also described in the structures of hydrous Zn-arsenates, namely legrandite $Zn_2[AsO_4](OH)(H_2O)$ (Pushcharovsky *et al*., 1971), adamite $Zn_2[AsO_4](OH)$ (Hawthorne, 1976) and the Cu, Zn-ordered analogue of the latter, zincolivenite $CuZn[AsO_4](OH)$ (Chukanov *et al*., 2007). In adamite and zincolivenite $ZnO_4(OH)$ trigonal bipyramids form the edge-sharing dimers as in zincomenite.

Discussion

Besides β-$ZnSeO_3$, two other polymorphous modifications of zinc selenite have been reported. The α-$ZnSeO_3$ form has been chemically characterized (Markovskii & Sapozhnikov, 1960) but its crystal structure has not been solved. The third, high-pressure modification of $ZnSeO_3$ (Kohn *et al*., 1976; Escamilla *et al*., 2002; Alonso *et al*., 2008) crystallizes in a distorted perovskite-like structure with Zn in octahedral coordination.

Since thermal behaviour of synthetic zinc selenite and its phase transformations have been explored by several authors (Markovskii & Yu., 1960; Gospodinov & Bogdanov, 1983; Gospodinov, 1984; Ebert *et al*., 1984; Verma, 1999; Vlaev *et al*., 2005), the occurrence of zincomenite in nature could open some insights into the genesis of selenite mineral associations in fumaroles of the Tolbachik volcano. β-$ZnSeO_3$ is considered to be the high-temperature modification of zinc selenite: it can be obtained from α-$ZnSeO_3$ upon heating of the latter to 285°C (Markovskii & Yu, 1960). However, the reverse transformation from beta- to alpha form of $ZnSeO_3$ does not occur, hence both synthetic β-$ZnSeO_3$ and zincomenite are stable at room temperature. The stability field of β-$ZnSeO_3$ extends until *ca*. 450 °C: at that temperature, gradual loss of SeO_2 becomes detectable and the products of isothermal decomposition contain significant amounts of ZnO (Gospodinov & Bogdanov, 1983; Gospodinov, 1984; Vlaev *et al*., 2005). At temperatures below 180–220 °C in H_2O-bearing systems (water vapour), hydrous zinc selenites are preferably formed (Charykova *et al*., 2014). The rate of thermal decomposition of β-$ZnSeO_3$ rapidly increases upon further increase of the temperature and becomes complete at 600 °C. Therefore, the thermal stability and hence, most probable formation temperature range of zincomenite can be roughly bracketed between 280 and 450 °C. Such estimation can be equally applied to the minerals closely associated with zincomenite. It is in agreement with temperatures measured *in situ* (see above). Zincomenite could be deposited directly from the gas phase as a volcanic sublimate: it is confirmed by the occurrence of its own well-shaped crystals (Fig. 1 and 2). In other cases, the new mineral (or its hypothetic proto-phase α-$ZnSeO_3$, if the process was occurring at a temperature lower than *ca*. 280 °C) was formed as the result of the reaction between fumarole gases and sofiite $Zn_2(SeO_3)Cl_2$ (Fig. 3).

According to Charykova & Krivovichev (2016), sofiite crystallizes directly from the gas phase at temperatures of 300–400 °C and atmospheric pressure. Upon cooling of the system, at temperatures not lower than *ca*. 280 °C sofiite could react with the SeO_2-bearing fumarolic gas, and zincomenite can be a solid product of this reaction: $Zn_2(SeO_3)Cl_2 + SeO_2 + H_2O \rightarrow 2ZnSeO_3 + 2HCl$. This assumption is indirectly confirmed by the fact that volcanic gas of fumaroles belonging to the Northern fumarole field of the First scoria cone of the NB GTFE is rich in HCl (Zelenski & Taran, 2012). Zincomenite is associated with flinteite K_2ZnCl_4 (its hypothetic protophase, a high-

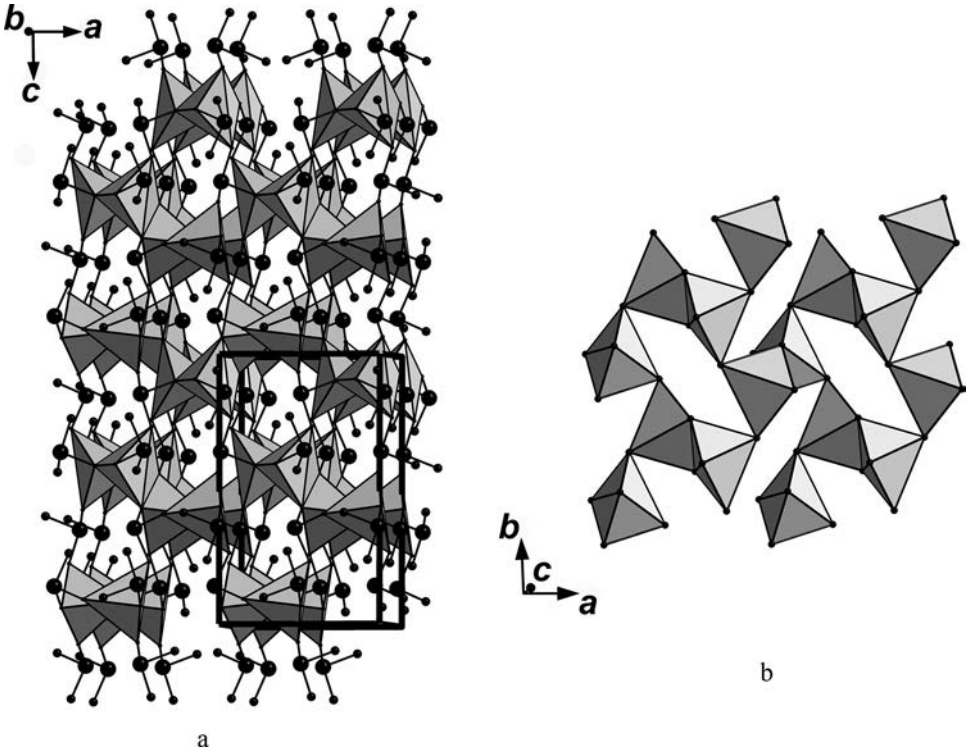

Fig. 5. The crystal structure of zincomenite: a – general view (the unit cell is outlined); b – the layer formed by ZnO_5 trigonal bipyramids. Zn-centred polyhedra are grey, Se atoms are large black circles connected with O atoms shown as small black circles.

temperature modification of dipotassium zinc chloride, can crystallize in the same temperature range: Pekov *et al*., 2015b) which allows us to assume the formation of this association as a result of alteration of sofiite by K- and Cl-bearing gas: $Zn_2(SeO_3)Cl_2 + 2K^+ + 2Cl^- \rightarrow ZnSeO_3 + K_2ZnCl_4$.

Acknowledgements: We thank Anna Garavelli and an anonymous referee for valuable comments. This study was supported by the Russian Science Foundation, grant no. 14-17-00048. The technical support by the SPbSU X-Ray Diffraction Research Resource Center in the XRD powder-diffraction studies is acknowledged.

References

Agilent Technologies (2012): CrysAlisPro software system, version 1.171.35.21. Agilent Technologies UK Ltd, Oxford, UK.

Alonso, J.A., Martinez Lope, M.J., De La Calle, C., Munoz, A., Moran, E., Demazeau, G. (2008): High-pressure synthesis and study of the crystal and magnetic structures of the distorted $SeMO_3$ (M = Mn, Co, Ni, Zn) perovskites. *J. Phys.: Conference Ser.*, **121**, 1–8.

Bachvarova-Nedelcheva, A., Iordanova, R., Dimitriev, Y. (2005): Synthesis of selenite glasses in air. *J. Univ. Chem. Technol. Metall.*, **40**, 315–318.

Bensch, W. & Günther, J.R. (1986): The crystal structure of beta-zinc selenite. *Z. Krist.*, **174**, 291–295.

Brese, N.E. & O'Keeffe, M. (1991): Bond-valence parameters for solids. *Acta Cryst.*, **B47**, 192–197.

Charykova, M.V. & Krivovichev, V.G. (2016): Thermodynamics of environmentally important natural and synthetic phases containing selenium. *in* "Biogenic—abiogenic interactions in natural and anthropogenic systems", Springer International Publishing Switzerland, Cham, 145–155.

Charykova, M.V., Fokina, E.L., Klimova, E.V., Krivovichev, V.G., Semenova, V.V. (2014): Thermodynamics of arsenates, selenites, and sulfates in the oxidation zone of sulfide ores. IX. Physicochemical formation conditions and thermal stability of zinc selenites. *Geol. Ore Deposits*, **56**, 546–552. [translated from: Charykova, M.V., Fokina, E.L., Klimova, E.V., Krivovichev, V.G. & Semenova, V.V. (2013): Thermodynamics of arsenates, selenites, and sulfates in the oxidation zone of sulfide ores. IX. Physicochemical formation conditions and thermal stability of zinc selenites. *Zapiski of the Russian Mineralogical Society*, **142**, 11-20 (in Russian)].

Chukanov, N.V. (2014): Infrared spectra of mineral species: Extended library. Springer Verlag, Dordrecht.

Chukanov, N.V. & Chervonnyi, A.D. (2016): Infrared spectroscopy of minerals and related compounds. Springer Verlag, Cham.

Chukanov, N.V., Pushcharovsky, D.Y., Zubkova, N.V., Pekov, I.V., Pasero, M., Merlino, S., Möckel, S., Rabadanov, M.K., Belakovskiy, D.I. (2007): Zincolivenite $CuZn(AsO_4)(OH)$: A new adamite-group mineral with ordered distribution of Cu and Zn. *Dokl. Earth Sci.*, **415**, 841–845.

Clark, R.C. & Reid, J.S. (1995): The analytical calculation of absorption correction in multifaceted crystals. *Acta Cryst.*, **A51**, 887–897.

Ebert, M., Mička, Z., Uchytilová, M. (1984): Zinc selenites: the solubility diagram and its use for the isolation of the compounds, their spectral features and thermal behaviour and the strength of bonds in them. *Coll. Czech. Chem. Commun*., **49**, 1653–1659.

Escamilla, R., Gallardo Amores, J.M., Moran, E., Alario-Franco, M.A. (2002): Crystal chemistry and magnetic properties of $SeCu_{1-x}Zn_xO_3$ ($0 \le x \le 1$) perovskites. *J. Solid State Chem*., **168**, 149–155.

Fedotov, S.A. & Markhinin, Y.K. eds. (1983): The great tolbachik fissure eruption. Cambridge Univ. Press, New York.

Georgiev, M., Marinova, D., Stoilova, D. (2010): Infrared spectroscopic studies of Tutton compounds. I. Vibrational behavior of XO_4^{2-} ions included in *Me*'$_2$*Me*"$(SeO_4)_2 \cdot 6H_2O$ (*Me*' = K, NH_4^+; *Me*" = Mg, Co, Ni, Cu, Zn). *J. Univ. Chem. Technol. Metall*., **45**, 75–82.

Gospodinov, G.G. (1984): Physico-chemical investigation of the system ZnO-SeO_2-H_2O and some properties of the compounds obtained. *Thermochim. Acta*, **77**, 439–444.

Gospodinov, G.G. & Bogdanov, B.G. (1983): Dimorphism of the anhydrous selenites of zinc, cadmium and mercury. *Thermochim. Acta*, **71**, 391–395.

Hawthorne, F.C. (1976): A refinement of the crystal structure of adamite. *Can. Mineral*., **14**, 143–148.

Hawthorne, F.C., Ercit, T.S., Groat, L.A. (1986): Structures of zinc selenite and copper selenite. *Acta Cryst*., **C42**, 1285–1287.

Kohn, K., Inoue, K., Horie, O., Akimoto, S. (1976): Crystal chemistry of $MSeO_3$ and $MTeO_3$ (M = Mg, Mn, Co, Ni, Cu and Zn). *J. Solid State Chem*., **18**, 27–37.

Krivovichev, S.V., Vergasova, L.P., Starova, G.L., Filatov, S.K., Britvin, S.N., Roberts, A.C., Steele, I.M. (2002): Burnsite, $KCdCu_7O_2(SeO_3)_2Cl_9$, a new mineral species from the Tolbachik Volcano, Kamchatka Peninsula, Russia. *Can. Mineral*., **40**, 1171–1175.

Markovskii, L.Y. & Yu., S. (1960): The different forms and some properties of neutral zinc selenite. *J. Struct. Chem*., **1**, 321–328.

Pekov, I.V., Zubkova, N.V., Pautov, L.A., Yapaskurt, V.O., Chukanov, N.V., Lykova, I.S., Britvin, S.N., Sidorov, E.G., Pushcharovsky, D.Y. (2015a): Chubarovite, $KZn_2(BO_3)Cl_2$, a new mineral species from the Tolbachik volcano, Kamchatka, Russia. *Can. Mineral*., **53**, 273–284.

Pekov, I.V., Zubkova, N.V., Yapaskurt, V.O., Britvin, S.N., Vigasina, M.F., Sidorov, E.G., Pushcharovsky, D.Y. (2015b): New zinc and potassium chlorides from fumaroles of the Tolbachik volcano, Kamchatka, Russia: mineral data and crystal chemistry. II. Flinteite, K_2ZnCl_4. *Eur. J. Mineral*., **27**, 581–588.

Pekov, I.V., Zubkova, N.V., Britvin, S.N., Yapaskurt, V.O., Chukanov, N.V., Lykova, I.S., Sidorov, E.G., Pushcharovsky, D.Y. (2015c): New zinc and potassium chlorides from fumaroles of the Tolbachik volcano, Kamchatka, Russia: mineral data and crystal chemistry. III. Cryobostryxite, $KZnCl_3 \cdot 2H_2O$. *Eur. J. Mineral*., **27**, 805–812.

Pushcharovsky, D.Y., Pobedimskaya, E.A., Belov, N.V. (1971): The crystal structure of legrandite $Zn_2(AsO_4)OH(H_2O)$. *Dokl. AN SSSR*, **198**, 1072–1075. (in Russian).

Serafimova, E.K., Semenova, T.F., Sulimova, N.V. (1994): The copper and lead minerals from ancient fumarole fields of Mountain 1004 (Kamchatka). *Vulkanol. Seismol*., **3**, 35–49. (in Russian).

Sheldrick, G.M. (2008): Short history of SHELX. *Acta Cryst. A*, **64**, 112–122.

Shuvalov, R.R., Vergasova, L.P., Semenova, T.F., Filatov, S.K., Krivovichev, S.V., Siidra, O.I., Rudashevsky, N.S. (2013): Prewittite, $KPb_{1.5}Cu_6Zn(SeO_3)_2O_2Cl_{10}$, a new mineral from Tolbachik fumaroles, Kamchatka Peninsula, Russia: description and crystal structure. *Am. Mineral*., **98**, 463–469.

Vergasova, L.P., Filatov, S.K., Semenova, T.F., Filosofova, T.M. (1989): Sofiite, $Zn_2(SeO_3)Cl_2$, a new mineral of volcanic exhalations. *Zapiski VMO*, **118**, 65–69. (in Russian).

Vergasova, L.P., Krivovichev, S.V., Britvin, S.N., Filatov, S.K., Burns, P.C., Ananiev, V.V. (2005): Allochalcoselite, $PbCu^+Cu^{2+}{}_5O_2(SeO_3)_2Cl_5$ – a new mineral from volcanic exhalations (Kamchatka Peninsula, Russia). *Zapiski RMO*, **134**, 70–73. (in Russian).

Vergasova, L.P., Krivovichev, S.V., Filatov, S.K., Britvin, S.N., Burns, P.C., Ananiev, V.V. (2007): Parageorgbokiite, β-$Cu_5O_2(SeO_3)_2Cl_2$ – a new mineral from volcanic exhalations (Kamchatka Peninsula, Russia). *Geol. Ore Dep*., **49**, 518–521.

Vergasova, L.P., Krivovichev, S.V., Semenova, T.F., Filatov, S.K., Ananiev, V.V. (1999b): Chloromenite, $Cu_9O_2(SeO_3)_4Cl_6$, a new mineral from the Tolbachik volcano, Kamchatka, Russia. *Eur. J. Mineral*., **11**, 119–123.

Vergasova, L.P., Semenova, T.F., Filatov, S.K., Krivovichev, S.V., Shuvalov, R.R., Ananiev, V.V. (1999a): Georgbokiite $Cu_5O_2(SeO_3)_2Cl_2$ – a new mineral from volcanic sublimates. *Dokl. Akad. Nauk SSSR*, **364**, 527–531. (in Russian).

Vergasova, L.P., Semenova, T.F., Krivovichev, S.V., Filatov, S.K., Zolotarev Jr., A.A., Ananiev, V.V. (2014): Nicksobolevite, $Cu_7(SeO_3)_3O_2Cl_6$, a new complex copper oxoselenite chloride from Tolbachik fumaroles, Kamchatka peninsula, Russia. *Eur. J. Mineral*., **26**, 439–449.

Vergasova, L.P., Semenova, T.F., Shuvalov, R.R., Filatov, S.K., Ananiev, V.V. (1997): Ilinskite, $NaCu_5O_2(SeO_3)_2Cl_3$ – a new mineral of volcanic exhalations. *Dokl. Akad. Nauk SSSR*, **353**, 641–644. (in Russian).

Verma, V.P. (1999): A review of synthetic, thermoanalytical, IR, Raman and X-ray studies on metal selenites. *Thermochim. Acta*, **327**, 63–102.

Vlaev, L.T., Georgieva, V.G., Gospodinov, G.G. (2005): Kinetics of isothermal decomposition of $ZnSeO_3$ and $CdSeO_3$. *J. Therm. Anal. Calorimetry*, **79**, 163–168.

Zelenski, M. & Taran, Y. (2012): Volcanic emissions of molecular chlorine. *Geochim. Cosmochim. Acta*, **87**, 210–226.

Received 15 March 2016
Modified version received 25 April 2016
Accepted 27 April 2016